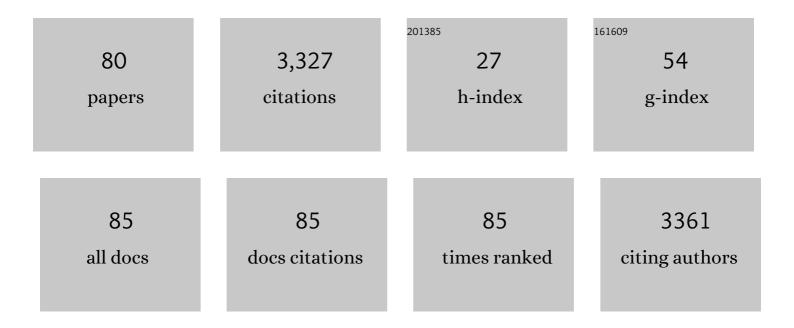


## List of Publications by Year in descending order

Source: https://exaly.com/author-pdf/7185715/publications.pdf Version: 2024-02-01



VAN V VII

#	Article	IF	CITATIONS
1	Improving <scp>ligandâ€ғanking</scp> of <scp>AutoDock</scp> Vina by changing the empirical parameters. Journal of Computational Chemistry, 2022, 43, 160-169.	1.5	19
2	Unbinding ligands from SARS-CoV-2 Mpro via umbrella sampling simulations. Royal Society Open Science, 2022, 9, 211480.	1.1	9
3	Insights into the binding and covalent inhibition mechanism of PF-07321332 to SARS-CoV-2 M <sup>pro</sup> . RSC Advances, 2022, 12, 3729-3737.	1.7	19
4	501Y.V2 spike protein resists the neutralizing antibody in atomistic simulations. Computational Biology and Chemistry, 2022, 97, 107636.	1.1	1
5	Effect of Cholesterol Molecules on Al $^2$ 1-42 Wild-Type and Mutants Trimers. Molecules, 2022, 27, 1395.	1.7	13
6	Umbrella Sampling-Based Method to Compute Ligand-Binding Affinity. Methods in Molecular Biology, 2022, 2385, 313-323.	0.4	5
7	Searching for AChE inhibitors from natural compounds by using machine learning and atomistic simulations. Journal of Molecular Graphics and Modelling, 2022, 115, 108230.	1.3	8
8	Identifying Possible AChE Inhibitors from Drug-like Molecules via Machine Learning and Experimental Studies. ACS Omega, 2022, 7, 20673-20682.	1.6	11
9	Estimating the <scp>ligandâ€binding</scp> affinity via <scp>λâ€dependent</scp> umbrella sampling simulations. Journal of Computational Chemistry, 2021, 42, 117-123.	1.5	14
10	Computational investigation of possible inhibitors of the winged-helix domain of MUS81. Journal of Molecular Graphics and Modelling, 2021, 103, 107771.	1.3	5
11	Binding of inhibitors to the monomeric and dimeric SARS-CoV-2 Mpro. RSC Advances, 2021, 11, 2926-2934.	1.7	19
12	Amyloid Oligomers: A Joint Experimental/Computational Perspective on Alzheimer's Disease, Parkinson's Disease, Type II Diabetes, and Amyotrophic Lateral Sclerosis. Chemical Reviews, 2021, 121, 2545-2647.	23.0	406
13	Cholesterol Molecules Alter the Energy Landscape of Small Aβ1–42 Oligomers. Journal of Physical Chemistry B, 2021, 125, 2299-2307.	1.2	12
14	Impact of the Rat R5G, Y10F, and H13R Mutations on Tetrameric Aβ42 β-Barrel in a Lipid Bilayer Membrane Model. Journal of Physical Chemistry B, 2021, 125, 3105-3113.	1.2	3
15	Benchmark of Popular Free Energy Approaches Revealing the Inhibitors Binding to SARS-CoV-2 Mpro. Journal of Chemical Information and Modeling, 2021, 61, 2302-2312.	2.5	66
16	Terahertz cut-wire-pair metamaterial absorber. Journal of Applied Physics, 2021, 130, .	1.1	4
17	Systematic Investigation of the Structure, Stability, and Spin Magnetic Moment of CrM <sub><i>n</i></sub> Clusters (M = Cu, Ag, Au, and <i>n</i> = 2–20) by DFT Calculations. ACS Omega, 2021, 6, 20341-20350.	1.6	9
18	Marine derivatives prevent <i>w</i> MUS81 <i>in silico</i> studies. Royal Society Open Science, 2021, 8, 210974.	1.1	5

VAN V VU

#	Article	IF	CITATIONS
19	Potential inhibitors for SARS-CoV-2 Mpro from marine compounds. RSC Advances, 2021, 11, 22206-22213.	1.7	8
20	Thermodynamics and kinetics in antibody resistance of the 501Y.V2 SARS-CoV-2 variant. RSC Advances, 2021, 11, 33438-33446.	1.7	3
21	Searching and designing potential inhibitors for SARS-CoV-2 Mpro from natural sources using atomistic and deep-learning calculations. RSC Advances, 2021, 11, 38495-38504.	1.7	11
22	Autodock Vina Adopts More Accurate Binding Poses but Autodock4 Forms Better Binding Affinity. Journal of Chemical Information and Modeling, 2020, 60, 204-211.	2.5	233
23	Oversampling Free Energy Perturbation Simulation in Determination of the Ligandâ€Binding Free Energy. Journal of Computational Chemistry, 2020, 41, 611-618.	1.5	30
24	Fabrication of superhydrophobic surface using one-step chemical treatment. Surfaces and Interfaces, 2020, 21, 100673.	1.5	9
25	Assessing potential inhibitors of SARS-CoV-2 main protease from available drugs using free energy perturbation simulations. RSC Advances, 2020, 10, 40284-40290.	1.7	21
26	How do magnetic, structural, and electronic criteria of aromaticity relate to HOMO – LUMO gap? An evaluation for graphene quantum dot and its derivatives. Chemical Physics, 2020, 539, 110951.	0.9	16
27	Rapid prediction of possible inhibitors for SARS-CoV-2 main protease using docking and FPL simulations. RSC Advances, 2020, 10, 31991-31996.	1.7	30
28	Computational Determination of Potential Inhibitors of SARS-CoV-2 Main Protease. Journal of Chemical Information and Modeling, 2020, 60, 5771-5780.	2.5	118
29	Impact of the Astaxanthin, Betanin, and EGCG Compounds on Small Oligomers of Amyloid Al² <sub>40</sub> Peptide. Journal of Chemical Information and Modeling, 2020, 60, 1399-1408.	2.5	17
30	Effective estimation of the inhibitor affinity of HIV-1 protease <i>via</i> a modified LIE approach. RSC Advances, 2020, 10, 7732-7739.	1.7	7
31	Impact of A2T and D23N Mutations on Tetrameric Aβ42 Barrel within a Dipalmitoylphosphatidylcholine Lipid Bilayer Membrane by Replica Exchange Molecular Dynamics. Journal of Physical Chemistry B, 2020, 124, 1175-1182.	1.2	18
32	Stability of Aβ11–40 Trimers with Parallel and Antiparallel β-Sheet Organizations in a Membrane-Mimicking Environment by Replica Exchange Molecular Dynamics Simulation. Journal of Physical Chemistry B, 2020, 124, 617-626.	1.2	21
33	Fine Tuning of the Copper Active Site in Polysaccharide Monooxygenases. Journal of Physical Chemistry B, 2020, 124, 1859-1865.	1.2	3
34	C-Terminal Plays as the Possible Nucleation of the Self-Aggregation of the S-Shape Aβ <sub>11–42</sub> Tetramer in Solution: Intensive MD Study. ACS Omega, 2019, 4, 11066-11073.	1.6	8
35	Interaction of carbohydrate binding module 20 with starch substrates. RSC Advances, 2019, 9, 24833-24842.	1.7	12
36	Tetrameric Aβ40 and Aβ42 β-Barrel Structures by Extensive Atomistic Simulations. II. In Aqueous Solution. Journal of Physical Chemistry B, 2019, 123, 6750-6756.	1.2	31

Van V Vu

#	Article	IF	CITATIONS
37	Prediction of AChE-ligand affinity using the umbrella sampling simulation. Journal of Molecular Graphics and Modelling, 2019, 93, 107441.	1.3	24
38	Substrate selectivity in starch polysaccharide monooxygenases. Journal of Biological Chemistry, 2019, 294, 12157-12166.	1.6	31
39	Adequate prediction for inhibitor affinity of Aβ <sub>40</sub> protofibril using the linear interaction energy method. RSC Advances, 2019, 9, 12455-12461.	1.7	16
40	Probable Transmembrane Amyloid α-Helix Bundles Capable of Conducting Ca <sup>2+</sup> Ions. Journal of Physical Chemistry B, 2019, 123, 2645-2653.	1.2	26
41	Tetrameric Aβ40 and Aβ42 β-Barrel Structures by Extensive Atomistic Simulations. I. In a Bilayer Mimicking a Neuronal Membrane. Journal of Physical Chemistry B, 2019, 123, 3643-3648.	1.2	42
42	Effective Estimation of Ligand-Binding Affinity Using Biased Sampling Method. ACS Omega, 2019, 4, 3887-3893.	1.6	52
43	In vitroandin silicodetermination of glutaminyl cyclase inhibitors. RSC Advances, 2019, 9, 29619-29627.	1.7	14
44	Influence of various force fields in estimating the binding affinity of acetylcholinesterase inhibitors using fast pulling of ligand scheme. Chemical Physics Letters, 2018, 701, 65-71.	1.2	12
45	Propafenone effects on the stable structures of AÎ <sup>2</sup> 16-22 system. Chemical Physics Letters, 2018, 696, 55-60.	1.2	6
46	Copper active site in polysaccharide monooxygenases. Coordination Chemistry Reviews, 2018, 368, 134-157.	9.5	47
47	Atomistic investigation of an Iowa Amyloid-Î <sup>2</sup> trimer in aqueous solution. RSC Advances, 2018, 8, 41705-41712.	1.7	9
48	Conjugated polymers: A systematic investigation of their electronic and geometric properties using density functional theory and semi-empirical methods. Synthetic Metals, 2018, 246, 128-136.	2.1	11
49	Etersalate prevents the formations of 6AÎ <sup>2</sup> 16-22 oligomer: An in silico study. PLoS ONE, 2018, 13, e0204026.	1.1	11
50	The influences of E22Q mutant on solvated 3Aβ 11-40 peptide: A REMD study. Journal of Molecular Graphics and Modelling, 2018, 83, 122-128.	1.3	6
51	Computational Investigations of the Transmembrane Italian-Mutant (E22K) 3A(eta_{11 - 40}) in Aqueous Solution. Communications in Physics, 2018, 28, 265.	0.0	3
52	Solution structure of the reduced active site of a starch-active polysaccharide monooxygenase from Neurospora crassa. Vietnam Journal of Science Technology and Engineering, 2018, 60, 9-12.	0.1	2
53	Fast pulling of ligand approach for the design of β-secretase 1 inhibitors. Chemical Physics Letters, 2017, 671, 142-146.	1.2	14
54	Replica exchange molecular dynamics study of the amyloid beta (11–40) trimer penetrating a membrane. RSC Advances, 2017, 7, 7346-7357.	1.7	38

Van V Vu

#	Article	IF	CITATIONS
55	Determination of the absolute binding free energies of HIV-1 protease inhibitors using non-equilibrium molecular dynamics simulations. Chemical Physics Letters, 2017, 676, 12-17.	1.2	27
56	Replica exchange molecular dynamics study of the truncated amyloid beta (11–40) trimer in solution. Physical Chemistry Chemical Physics, 2017, 19, 1909-1919.	1.3	36
57	The Effects of A21G Mutation on Transmembrane Amyloid Beta (11–40) Trimer: An <i>In Silico</i> Study. Journal of Physical Chemistry B, 2017, 121, 8467-8474.	1.2	24
58	Evaluation of the absolute affinity of neuraminidase inhibitor using steered molecular dynamics simulations. Journal of Molecular Graphics and Modelling, 2017, 77, 137-142.	1.3	12
59	In silico studies of solvated F19W amyloid β (11–40) trimer. RSC Advances, 2017, 7, 42379-42386.	1.7	15
60	EGCG inhibits the oligomerization of amyloid beta (16-22) hexamer: Theoretical studies. Journal of Molecular Graphics and Modelling, 2017, 76, 1-10.	1.3	38
61	X-ray absorption spectroscopic characterization of the diferric-peroxo intermediate of human deoxyhypusine hydroxylase in the presence of its substrate eIF5a. Journal of Biological Inorganic Chemistry, 2016, 21, 605-618.	1.1	21
62	Starch-degrading polysaccharide monooxygenases. Cellular and Molecular Life Sciences, 2016, 73, 2809-2819.	2.4	33
63	Fast and accurate determination of the relative binding affinities of small compounds to HIV-1 protease using non-equilibrium work. Journal of Computational Chemistry, 2016, 37, 2734-2742.	1.5	70
64	Theoretical study of the interactions between the first transmembrane segment of NS2 protein and a POPC lipid bilayer. Biophysical Chemistry, 2016, 217, 1-7.	1.5	8
65	Anti-arrhythmic Medication Propafenone a Potential Drug for Alzheimer's Disease Inhibiting Aggregation of Aβ: In Silico and in Vitro Studies. Journal of Chemical Information and Modeling, 2016, 56, 1344-1356.	2.5	41
66	Estimation of the Binding Free Energy of AC1NX476 toÂHIVâ€1 Protease Wild Type and Mutations Using FreeÂEnergy Perturbation Method. Chemical Biology and Drug Design, 2015, 86, 546-558.	1.5	24
67	An Unusual Peroxo Intermediate of the Arylamine Oxygenase of the Chloramphenicol Biosynthetic Pathway. Journal of the American Chemical Society, 2015, 137, 1608-1617.	6.6	71
68	Cellulose Degradation by Polysaccharide Monooxygenases. Annual Review of Biochemistry, 2015, 84, 923-946.	5.0	246
69	Determinants of Regioselective Hydroxylation in the Fungal Polysaccharide Monooxygenases. Journal of the American Chemical Society, 2014, 136, 562-565.	6.6	198
70	A family of starch-active polysaccharide monooxygenases. Proceedings of the National Academy of Sciences of the United States of America, 2014, 111, 13822-13827.	3.3	222
71	Effect of the Tottori Familial Disease Mutation (D7N) on the Monomers and Dimers of Al² <sub>40</sub> and Al² <sub>42</sub> . ACS Chemical Neuroscience, 2013, 4, 1446-1457.	1.7	83
72	In silico and in vitro characterization of anti-amyloidogenic activity of vitamin K3 analogues for Alzheimer's disease. Biochimica Et Biophysica Acta - General Subjects, 2013, 1830, 2960-2969.	1.1	38

Van V Vu

#	Article	IF	CITATIONS
73	Top-leads from natural products for treatment of Alzheimer's disease: docking and molecular dynamics study. Molecular Simulation, 2013, 39, 279-291.	0.9	50
74	Oligomerization of Peptides LVEALYL and RGFFYT and Their Binding Affinity to Insulin. PLoS ONE, 2013, 8, e65358.	1.1	21
75	A mononuclear carboxylate-rich oxoiron(iv) complex: a structural and functional mimic of TauD intermediate â€J'. Chemical Science, 2012, 3, 1680.	3.7	40
76	Curcumin Binds to Aβ <sub>1–40</sub> Peptides and Fibrils Stronger Than Ibuprofen and Naproxen. Journal of Physical Chemistry B, 2012, 116, 10165-10175.	1.2	85
77	Active-Site Structure of a β-Hydroxylase in Antibiotic Biosynthesis. Journal of the American Chemical Society, 2011, 133, 6938-6941.	6.6	21
78	Inhibition of Aggregation of Amyloid Peptides by Beta-Sheet Breaker Peptides and Their Binding Affinity. Journal of Physical Chemistry B, 2011, 115, 7433-7446.	1.2	173
79	Human deoxyhypusine hydroxylase, an enzyme involved in regulating cell growth, activates O <sub>2</sub> with a nonheme diiron center. Proceedings of the National Academy of Sciences of the United States of America, 2009, 106, 14814-14819.	3.3	105
80	Characterization of Two Distinct Adducts in the Reaction of a Nonheme Diiron(II) Complex with O <sub>2</sub> . Inorganic Chemistry, 2009, 48, 8325-8336.	1.9	33